PHYSICAL REVIEW B (2004) 70(21):214517.

Universal intrinsic scale of the hole concentration in high-T_c cuprates

Honma T, Hor PH, Hsieh HH, Tanimoto M

Universal intrinsic scale of the hole concentration in high-T_c cuprates

T. Honma*
Department of Physics and Texas Center for Superconductivity and Advanced Materials, University of Houston, Houston, Texas 77204-5005, USA
and Department of Physics, Asahikawa Medical College, Asahikawa 078-8510, Japan

P. H. Hor
Department of Physics and Texas Center for Superconductivity and Advanced Materials, University of Houston, Houston, Texas 77204-5005, USA

H. H. Hsieh
Department of Physics and Texas Center for Superconductivity and Advanced Materials, University of Houston, Houston, Texas 77204-5005, USA
and Synchrotron Radiation Research Center, Hsinchu, Taiwan 30077, Republic of China

M. Tanimoto
Department of Physics, Asahikawa Medical College, Asahikawa 078-8510, Japan
(Received 2 June 2004; revised manuscript received 20 September 2004; published 14 December 2004)

We have measured thermoelectric power (TEP) as a function of hole concentration per CuO_2 layer P_{pl} in $Y_{1-x}Ca_xBa_2Cu_3O_6$ ($P_{pl}=x/2$) with no oxygen in the Cu-O chain layer. The room-temperature TEP as a function of P_{pl}, $S^{290}(P_{pl})$, of $Y_{1-x}Ca_xBa_2Cu_3O_6$ behaves identically to that of $La_{2-z}Sr_zCuO_4$ ($P_{pl}=z$). We argue that $S^{290}(P_{pl})$ represents a measure of the intrinsic equilibrium electronic states of doped holes and, therefore, can be used as a common scale for the carrier concentrations of layered cuprates. We shows that the P_{pl} determined by this new universal scale is consistent with both hole concentration microscopically determined by NQR and the hole concentration macroscopically determined by the formal valency of Cu. We find two characteristic scaling temperatures, T_S^* and T_{S2}^*, in the TEP versus temperature curves that change systematically with doping. Based on the universal scale, we uncover a universal phase diagram in which almost all the experimentally determined pseudogap temperatures as a function of P_{pl} fall on two common curves; *lower pseudogap* temperature defined by the T_S^* versus P_{pl} curve and *upper pseudogap* temperature defined by the T_{S2}^* versus P_{pl} curve. We find that while pseudogaps are intrinsic properties of doped holes of a single CuO_2 layer for all high-T_c cuprates, T_c depends on the number of layers, therefore, the inter layer coupling, in each individual system.

DOI: 10.1103/PhysRevB.70.214517 PACS number(s): 74.25.Fy, 74.25.Dw, 74.62.Dh, 74.72.−h

I. INTRODUCTION

Understanding some of the peculiar properties of the high-temperature superconductors (HTSCs) is one of challenging problems in condensed matter physics. Especially in the underdoped region, not only the unusually high-superconducting transition temperature (T_c) but also many normal state properties have defied our current knowledge of metal. The tremendous experimental results have been accumulated since the discovery of HTSC in 1986. Unfortunately, due to both experimental and material constraints, many high-quality data were collected on different materials. For instance, neutron scattering experiments require very large single crystals and, therefore, have almost exclusively been done on $YBa_2Cu_3O_y$ (Y123) and $La_{2-z}Sr_zCuO_4$ (LS214) so that big crystals can be grown. Angle-resolved photoemission spectroscopy (ARPES) and scanning tunneling microscopy (STM), which are sensitive to surface conditions, have been performed mainly on $Bi_2Sr_2CaCu_2O_y$ so that a virgin surface can be obtained by cleavage. On the other hand, resistivity ρ, Hall coefficient R_H, and thermoelectric power (TEP) S have been measured on almost all HTSCs. It will be most fruitful if different measurements done on different materials can be compared and analyzed on a common ground, say, hole concentration per CuO_2 layer P_{pl}. P_{pl} can be determined by Sr content z ($P_{pl}=z$) in $La_{2-z}Sr_zCuO_4$ with only cation doping, but it is hard to determine P_{pl} unambiguously in the other systems with anion doping. If P_{pl} can be determined by either one of ρ, R_H, or S, then almost all the available data can be compared quantitatively and analyzed on a common physical ground. Establishing a scale based on TEP is very powerful because the S of HTSC is not sensitive to both the grain boundary and porosity effects.[1] Therefore, with some precautions both single-crystal and polycrystalline data can be compared.

The underdoped HTSC is characterized by a gaplike anomaly appearing below a characteristic temperature, the so-called pseudogap temperature. The pseudogap behavior was first observed in ^{89}Y NMR Knight shift ΔK and in the ^{63}Cu spin-lattice relaxation rate $^{63}(T_1T)^{-1}$ (Ref. 2). It also showed up as an anomaly in the ρ and R_H versus temperature curves.[3,4] Subsequently, the pseudogap behavior has been observed in many experimental probes, such as far infrared,[5] ARPES,[6] TEP,[7] specific heat,[8,9] time-resolved quasiparticle

relaxation (QPR) measurement,[10] and so on. The pseudogap temperature systematically varies with cation or anion doping in individual systems. However, for the above reason, these pseudogap temperatures cannot be compared based on the hole concentration. In such a situation, the room-temperature TEP (S^{290}) was proposed to be useful for determining P_{pl}.[11] According to this scale, the pseudogap behavior is summarized on the phase diagram that the pseudogap temperature falls from higher temperature at lower hole concentration to zero at a critical hole concentration across the T_c curve.[12] On the other hand, the result of ARPES suggests that the pseudogap temperature does not cross the T_c curve, but smoothly merges with T_c on the slightly overdoped side.[6]

For LS214 system, T_c appears at $P_{pl} \approx 0.06$, passes a maximum $T_c(T_c^{max})$ at $P_{pl} \approx 0.16$, and, finally, falls to zero at $P_{pl} \approx 0.27$. It was approximated by a parabolic curve[13]

$$T_c/T_c^{max} = 1 - 82.6(P_{pl} - 0.16)^2. \quad (1)$$

Although Eq. (1) can be conveniently used to estimate P_{pl} for the systems with similar parabolic variation of T_c, it cannot be used for the systems with a complex variation of T_c, such as Y123. P_{pl} of Y123 was estimated from the bond valence sum (BVS) analysis, which relied on accurate knowledge of interatomic bond lengths.[14] Later, it was shown that, for some HTSCs, S^{290} can be used to estimate P_{pl} consistent with that determined by either Eq. (1) or BVS analysis.[11] The following empirical formula has been proposed:[15]

$$S^{290}[\mu V/K] = \begin{cases} 372\ \exp(-32.4P_{pl}) & (0.00 < P_{pl} < 0.05) \\ 992\ \exp(-38.1P_{pl}) & (0.05 < P_{pl} < 0.155) \\ 24.2 - 139P_{pl} & (0.155 < P_{pl}). \end{cases} \quad (2)$$

Equation (2) has been widely used with the distinct advantages that S^{290} is material independent. Therefore, it can be used to compare physical properties as a function of P_{pl} of very different HTSCs. But, there are still difficulties in using Eq. (2). For instance, there is no reason why the optimal P_{pl}, where T_c^{max} appears, should be universally ~ 0.16 for HTSC as has already been questioned in Ref. 16. It is also not trivial to apply BVS to determine P_{pl} for systems with internal strain due to the CuO chain structure, such as Y123.[17] Furthermore, it is reported that, for LS214,[11] $(Ca_xLa_{1-x})(Ba_{1.75-x}La_{0.25+x})Cu_3O_y$ (C_xLBLC),[18] and $Bi_2Sr_{2-x}La_xCuO_y$ (Bi2201),[19] P_{pl}'s determined by Eq. (1) are not consistent with those determined by Eq. (2).

$Y_{1-x}Ca_xBa_2Cu_3O_6$ (YC1236) without CuO chain has two equivalent CuO_2 planes, therefore, the P_{pl} can be determined unambiguously by Ca content x as $P_{pl}=x/2$. Different from the well-known and widely used empirical correlation between S^{290} and P_{pl} (Ref. 11), we find that $S^{290}(P_{pl})$ for YC1236 behaves identically to that for LS214. Since the crystal structure for YC1236 is very different from that for LS214, we argue that this different correlation of S^{290} can be used as an intrinsic scale of P_{pl} for different HTSC cuprates. We demonstrate that this conjecture seems to work by uncovering a universal phase diagram of the pseudogap and superconductivity. We find that while the pseudogap phase is an intrinsic property to single CuO_2 layer, the bulk T_c seems to be governed exclusively by the interlayer coupling.

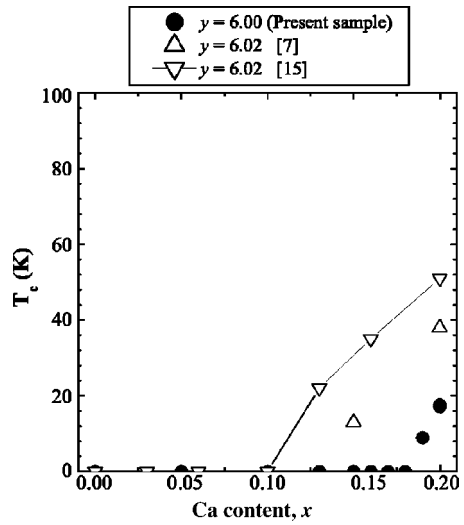

FIG. 1. Superconducting transition temperature (T_c) as a function of Ca doping level for the double-layer $Y_{1-x}Ca_xBa_2Cu_3O_y$. The data for the samples with $y=6.00$ are present work. The others are data reported in the literature (Refs. 7 and 15). The solid lines are guide to the eyes.

II. EXPERIMENTAL

$Y_{1-x}Ca_xBa_2Cu_3O_6$ with different Ca contents of $x=0.05$, 0.10, 0.13, 0.15, 0.17, 0.18, 0.19, 0.20, and 0.22 were prepared by causing a solid-state reaction in a proportioned mixture of Y_2O_3 (5N), $CaCO_3$ (5N), $BaCO_3$ (5N), and CuO (4N). These powders were ground, pressed, and fired in flowing O_2 at 900 °C for 6 hr. This process was repeated several times. For the final firing, two pellets with ~ 0.5 g each were fired for $10 \sim 15$ hr in flowing O_2 at $920 \sim 940$ °C. The O_2 gas was exchanged into Ar gas (99.9995%) at the high temperature, before in the furnace with flowing Ar gas the samples were annealed at 750 °C and cooled to room temperature. The oxygen content y was confirmed to be 6.00 ± 0.01 by using an iodometric titration technique under Ar gas. The prepared $Y_{1-x}Ca_xBa_2Cu_3O_6$ samples with $x \leqslant 0.22$ were identified as a single-phase by examining the x-ray powder diffraction pattern. The $Y_{0.75}Ca_{0.25}Ba_2Cu_3O_6$ showed some minor second phase, although the main peak of the second phase was below 1% for the main peak of the 123 phase. The density of all prepared samples was over 80% of the theoretical density. Figure 1 shows the Ca content dependence of T_c with previous reported results.[7,15] The prepared samples show no superconducting transition until $x=0.18$, while the superconductivity appears above ~ 0.125 in some other group's samples with $y=6.02$.[7,15] Accordingly, the chain-site oxygen of the present samples is confirmed to be adequately reduced. The TEP was measured by an ac method with a low-frequency (33 mHz) heating technique.[20]

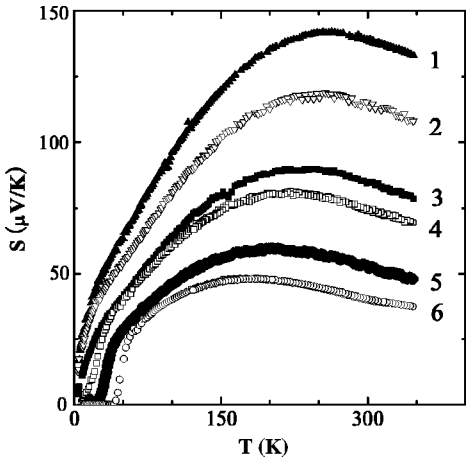

FIG. 2. The evolution of $S(T)$ for different Ca contents of the double-layer $Y_{1-x}Ca_xBa_2Cu_3O_6$. The Ca contents of samples 1–6 are 0.10, 0.13, 0.15, 0.18, 0.20, and 0.22, respectively.

III. RESULTS AND DISCUSSION

A. Temperature dependence of TEP for $Y_{1-x}Ca_xBa_2Cu_3O_6$

Figure 2 shows the typical T dependence of TEP for a series of fully deoxygenated $Y_{1-x}Ca_xBa_2Cu_3O_6$ with $0.05 \leqslant x \leqslant 0.22$. The oxygen content is fixed to be 6.00 ± 0.01 here. Typically, upon increasing temperature T, positive S rises toward a broad peak at a temperature T_S^* and S decreases almost linearly for $T > T_S^*$. T_S^* was reported to be closely related to pseudogap temperature.[7] The T dependence of TEP, $S(T)$, systematically changes with Ca doping. T_S^* becomes lower with Ca doping, and the magnitude of TEP decreases. The observed $S(T)$ is very similar to that reported in LS214 (Refs. 21–27), $C_{0.4}$LBLC (Ref. 18), and $CaLaBaCu_3O_y$ (CLBC) (Ref. 28) without ordered CuO chain. Thus, it is confirmed that there is no significant chain contribution to TEP.[7]

$S(T)$ can be well scaled by the value S^* and temperature T_S^* of the peak as shown in Fig. 3. S/S^* can be fitted to a log T law for $0.3 < T/T_S^* < 0.8$ as shown in the inset. We confirmed that $S(T)$ data of $Bi_2Sr_2Ca_{1-x}Y_xCu_2O_y$(Bi2212) (Ref. 29), CLBC (Ref. 28), and $C_{0.4}$LBLC (Ref. 18) also

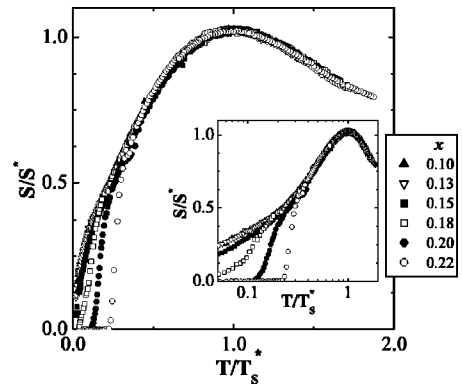

FIG. 3. S/S^* as a function of T/T_S^* for different Ca contents of the double-layer $Y_{1-x}Ca_xBa_2Cu_3O_6$. The inset shows S/S^* versus T/T_S^* on the logarithmic scale.

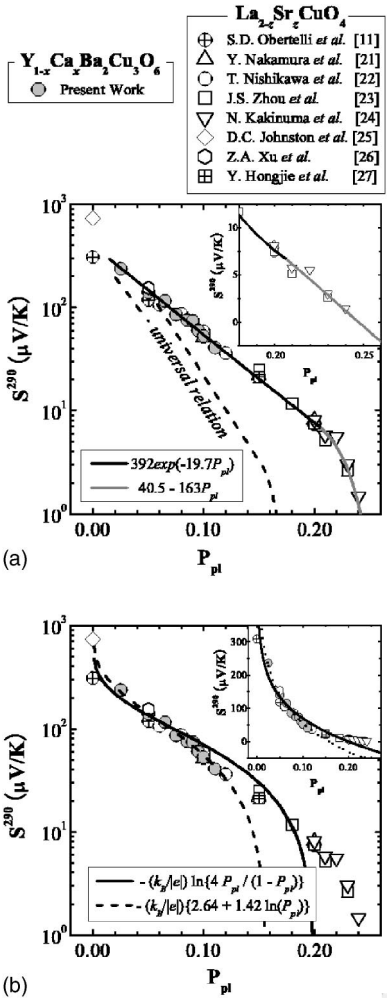

FIG. 4. S^{290} on the logarithmic scale versus P_{pl} for YC1236 and LS214. Inset: S^{290} on the linear scale versus P_{pl}. (a) The long dashed line shows Eq. (2) (Ref. 11). The black solid line and gray solid line show the Formula (3a) and (3b), respectively. (b) The solid line shows Eq. (4) (Ref. 36). The dashed line shows Eq. (5b) at 290 K (Ref. 38).

show the same scaling behavior by using the reported $S(T)$ data. Log T behavior for $T < T_S^*$ was reported in CLBC (Ref. 28) and $YBa_2Cu_3O_y$ ($y \leqslant 6.48$) (Ref. 11). Similar scaling behavior was also reported in the single-layer LS214, double-layer Y123 ($y \leqslant 6.65$), and Bi2212 (Refs. 30 and 31). Since all the above observations were done on samples without ordered CuO chains like Y123, we conclude that the broad peak at T_S^*, log T dependence for $T < T_S^*$ and T linear behavior for $T > T_S^*$ are intrinsic characteristic TEP properties of doped holes in the CuO_2 layer. As the superconductivity appears with doping, the scaled curve of S/S^* versus T/T_S^* can be cut off at the low-temperature side, as shown in Fig. 3. Accordingly, in the highly doped samples, the scaled curve for TEP could lose the log T behavior by the developement of the superconductivity. The schematic picture was shown in Fig. 1 of Ref. 7. In fact, such variation of $S(T)$ with doping was observed in Bi2212 (Ref. 31).

In $HgBa_2CuO_{4+\delta}$ (Hg1201), the $S(T)$ was well scaled by the temperature, where starts to decrease linearly with in-

creasing T, and the value at the temperature.[33] Similar scaling was reported also in Bi2212 (Ref. 34). Another characteristic temperature $T_{S2}^{*}(>T_{S}^{*})$ for TEP is reported in Zn-substituted Y123 (Ref. 32). The $S(T<T_{S2}^{*})$ is suppressed by Zn substitution, while the $S(T>T_{S2}^{*})$ does not depend on Zn substitution. Recently, the temperature used for another scaling method is reported to be just equal to the T_{S2}^{*}.[35] Therefore, the $S(T)$ can be characterized by two temperatures, T_{S}^{*} where $S(T)$ has a maximum and T_{S2}^{*} where $S(T)$ becomes sensitive to Zn substitution. We will discuss that both T_{S}^{*} and T_{S2}^{*} are related to the pseudogap in Sec. III B.

B. Room-temperature (RT) scale for hole concentration

Figure 4(a) shows S^{290} on the logarithmic scale as a function of P_{pl}. The closed circles represent the S^{290} for the fully deoxygenated samples of $Y_{1-x}Ca_xBa_2Cu_3O_6$ with $0.05\leqslant x\leqslant 0.22$. The P_{pl} can be determined unambiguously by Ca content x as $P_{pl}=x/2$, since YC1236 has two equivalent CuO_2 planes without CuO chain. For the comparison, the reported results of S^{290} in LS214 are represented by various different symbols,[11,21–27] and the universal curve proposed in Ref. 15 is shown as the long dashed line. We find that the observed $\log(S^{290})$ of YC1236 varies linearly with P_{pl} and does not follow the universal line. This relation can be represented by Eq. (3a). It can be clearly seen that S^{290} of $La_{2-z}Sr_zCuO_4$ with $0.05\leqslant z\leqslant 0.21$ fall exactly on the same curve as $S^{290}(P_{pl})$ for YC1236. For $P_{pl}>0.21$, $S^{290}(P_{pl})$ of LS214 changes from exponential to linear in P_{pl} as shown in the inset of Fig. 4(a). In the pure La_2CuO_4, there is the large scattering of S^{290} as shown in Fig. 4(a). $S^{290}(P_{pl})$ of the double-layer YC1236 is identical to that of the single-layer LS214, in spite of the difference between YC1236 and LS214 in the crystal structure, which leads us to conjecture that the present relation for $S^{290}(P_{pl})$ can serve as a universal scale of P_{pl} for layered HTSC with equivalent CuO_2 layers[39]

$$S^{290}[\mu V/K]=\begin{cases}392\ \exp(-19.7P_{pl}) & (0.02\leqslant P_{pl}\leqslant 0.21) \quad (3a)\\ 40.5-163P_{pl} & (0.21<P_{pl}). \quad (3b)\end{cases}$$

In Ref. 11, the $S^{290}(P_{pl})$ of $La_{2-z}Sr_zCuO_4$ did not follow Eq. (2). Two possibilities were pointed out.[11] The deviation may arise from scattering effects associated with the increasing concentration of oxygen vacancies within the CuO_2 layers, which occur especially for $z>0.12$. Structural instabilities that are related to the orthorhombic-tetragonal transition may have some effect. Since we know that YC1236 shows the tetragonal symmetry at room temperature[40] and the oxygen content is fixed at 6.00 ± 0.01, the identical $S^{290}(P_{pl})$ behaviors for both YC1236 and LS214 have effectively ruled out both possibilities.

Here, we compare the $S^{290}(P_{pl})$ that we used to construct our universal scale with some theoretical works in HTSC. First, Cooper *et al.* found that the room-temperature TEP observed in LS214 can be semiquantitaively explained by a modified Heikes formula based on hopping in a strongly Coulomb correlated system[36]

$$S(P_{pl})=-\frac{k_B}{|e|}\ln\frac{2P_{pl}}{1-P_{pl}}-\frac{k_B}{|e|}\ln 2, \quad (4)$$

where e is the electronic charge and k_B is the Boltzmann constant. The S arises from the Heikes formula, $-(k_B/|e|)\ln[P_{pl}/(1-P_{pl})]$ and a spin entropy term, $-(k_B/|e|)\ln 2$, with an orbital degeneracy term, $-(k_B/|e|)\ln 2$. The experiment data up to $P_{pl}\approx 0.2$ can be represented by Eq. (4) as shown in Fig. 4(b). However, no magnetic field dependence of TEP was observed, in spite of the expectation of the disappearance of the spin entropy term under the magnetic field.[37]

According to the Nagaosa-Lee model, using a gauge-field theory for a uniform-resonating valance-band (RVB) state,[38] the S is represented by a sum of fermion contribution, which is proportional to T, and boson contribution, which is proportional to $[1-\ln(2\pi P_{pl}/mk_BT)]$. The total S can be represented by Eq. (5a). The expression can be simplified as shown in Eq. (5b)

$$S(T,P_{pl})\sim\frac{k_B}{|e|}\left(1-\frac{k_B}{E_F}T-\ln\frac{2\pi P_{pl}}{mk_BT}\right), \quad (5a)$$

$$S(T,P_{pl})=\frac{k_B}{|e|}(a_0+a_1T+a_2\ln T+a_3\ln P_{pl}), \quad (5b)$$

where m is the effective mass and a_0, a_1, a_2, and a_3 are adjustable parameters. Equation (5b) is qualitatively consistent with the observed T dependence of TEP at a fixed hole concentration. The calculated TEP at 290 K, shown in Fig. 4(b), is consistent with the experiment data up to $P_{pl}\sim 0.12$. For $P_{pl}>0.12$, the calculated S is smaller than and increasingly deviates from S^{290} with doping.

Although the present Eqs. (3a) and (3b) are still empirical rules, it is found that the present equation is not artificial by comparison to the calculated results of the both models. We expect that a completed theory of high T_c should be able to account for the S^{290} versus P_{pl} curve over the whole doping region. Without even a working phenomenological theory, we resort to the same empirical approach and further check the validity of Eqs. (3a) and (3b) by showing that indeed, if

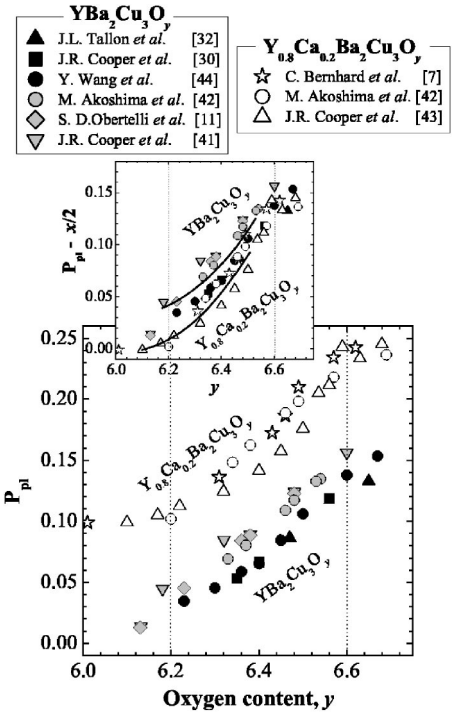

FIG. 5. P_{pl} determined from S^{290} as a function of oxygen-content, y in $Y_{1-x}Ca_xBa_2Cu_3O_y$. The inset shows the effective hole concentration $(P_{pl}-x/2)$ by the oxygen doping alone. The solid lines are a guide to the eyes.

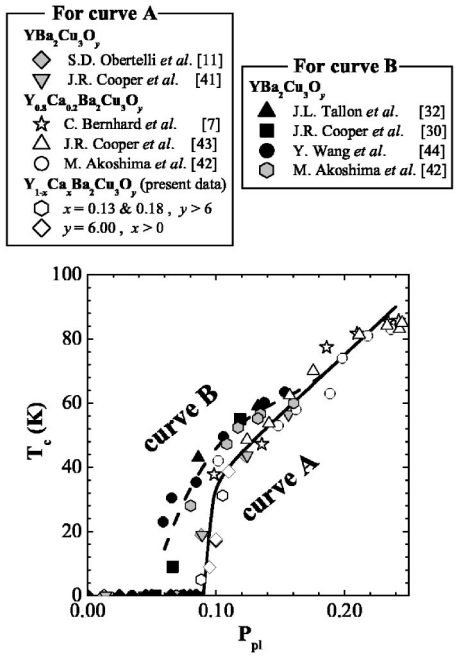

FIG. 6. T_c as a function of P_{pl} in $Y_{1-x}Ca_xBa_2Cu_3O_y$. The solid and dashed lines are a guide to the eyes for the curve A and curve B, respectively.

applying our universal scale to different material systems, physically meaningful comparisons and conclusions can be achieved.

C. Application of RT scale to $Y_{1-x}Ca_xBa_2Cu_3O_y$

Many TEP data for $Y_{1-x}Ca_xBa_2Cu_3O_y$ have been reported.[7,11,30,32,41–44] The anisotropy of the in-plane resistivity becomes significant when $y \approx 6.68$ in $YBa_2Cu_3O_y$ (Ref. 3). Therefore, we assume that the Y123 below $y \approx 6.68$ does not have the conductive chain or chain contribution to the transport property. Consequently, for the Y123 systems, the RT scale for the TEP was applied to the samples up to $y \approx 6.68$.

Figure 5 shows the P_{pl} determined from S^{290} as a function of oxygen content for $Y_{1-x}Ca_xBa_2Cu_3O_y$. The P_{pl}'s for $YBa_2Cu_3O_y$ are plotted by the closed black and gray symbols. The P_{pl}'s for $Y_{0.8}Ca_{0.2}Ba_2Cu_3O_y$ are plotted by the open symbols. In $YBa_2Cu_3O_y$, the hole carrier appears by oxygen doping beyond $y \approx 6.15$. There seems to be a threshold of the oxygen content for generating the hole carriers. Above $y \approx 6.2$, the hole carriers increase with oxygen doping. The $P_{pl}(y)$ curve trend is to divide into two curves in the range of $6.2 < y < 6.6$. The splitting of $P_{pl}(y)$ curve may be related to the formation of the CuO chain structure or the inhomogeneity of oxygen distribution on the CuO chain site. The Ca-doped Y123 shows a slightly different behavior compared to that for Y123. In $Y_{0.8}Ca_{0.2}Ba_2Cu_3O_y$, up to $y \approx 6.2$, the P_{pl} is almost 0.10, equal to the hole concentration generated by Ca doping of 0.20. This suggests the hole carriers are exclusively generated through the Ca doping. Above $y \approx 6.2$, the hole carriers increase almost linearly with oxygen doping. This is due to the generation of the hole carriers by oxygen doping. But, there is no threshold behavior due to oxygen doping. The $P_{pl}(y)$ curve trends to divide into two curves like Y123. In YC1236, the hole carrier can be generated even by slight Ca doping as shown in Fig. 4. The creation of hole carrier by oxygen doping may need the adequate oxygen content or threshold of hole carrier. The inset of Fig. 5 shows the effective hole concentration $(P_{pl}-x/2)$ due to oxygen doping alone. Although there is some scattering, the generation of hole carrier by oxygen doping is found to be slightly suppressed in the Ca-doped samples. The orthorhombic-tetragonal transition occurs in the range of $6.3 \lesssim y \lesssim 6.5$ (Refs. 42 and 45). The Ca doping may influence the formation of the microscopic CuO chain ordering. In the CLBC and C_xLBLC with significant Ca doping, there is no ordered CuO chain like Y123 (Ref. 7).

Figure 6 shows the T_c as a function of P_{pl} for $Y_{1-x}Ca_xBa_2Cu_3O_y$. There are two T_c versus P_{pl} curves. One is that the T_c appears at $P_{pl} \approx 0.09$ and increases linearly with P_{pl} for $P_{pl} \geqslant 0.1$ (curve A). The other is that the T_c appears at $P_{pl} \approx 0.06$ and merges into the curve A around ~ 0.18 (curve B). The curve A includes the $T_c(P_{pl})$ for YC1236 without CuO chain and $Y_{0.8}Ca_{0.2}Ba_2Cu_3O_y$ with $y < 6.6$. Further, the $T_c(P_{pl})$ for CLBC and C_xLBLC without ordered chain also follows the curve A.[18,28] In the curve A, two data for Y123 are included. The samples for these data were prepared over 10 years ago. It is well known that tuning the oxygen content using the quenching technique often leads to a large degree of in-plane disorder, which causes localization and strong T_c suppression.[44] The disorder can be removed by low-T annealing because the low-T annealing causes the oxygen-

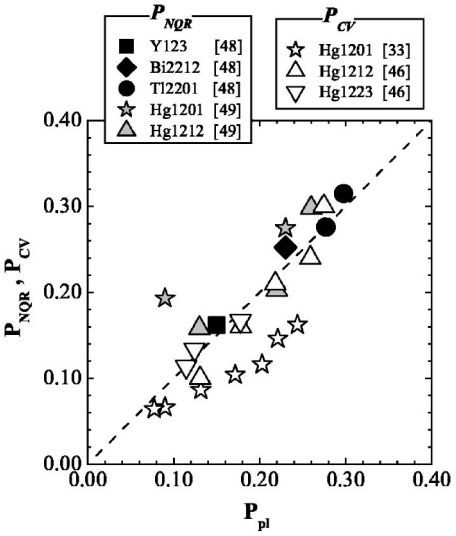

FIG. 7. P_{pl} determined from TEP by the present scale versus P_{NQR} determined from NQR and P_{CV} determined from Cu valency. The dashed line shows $P_{pl} = P_{NQR} = P_{CV}$.

rearrangement forming CuO chains.[45] The data from the latest Y123 samples fall on curve B. The Y123 data on curve A may have some disorder within the CuO chain layers, although it does not have the macroscopic chain ordering. Accordingly, curve A is for the samples with no chain or disordered chain fragments and curve B is for the samples with the relatively aligned chain fragments. In $Y_{0.8}Ca_{0.2}Ba_2Cu_3O_y$ with $y \approx 6.5$, the P_{pl} is ~ 0.20 and it shows the tetragonal symmetry.[42] The curve B merges into curve A at $P_{pl} \approx 0.18$. The anisotropy of the in-plane resistivity of the pure $YBa_2Cu_3O_y$ becomes significantly above $y \approx 6.68$ ($P_{pl} \approx 0.16$),[3] although the orthorhombic-tetragonal transition occurs at $y = 6.3 \sim 6.5$ ($P_{pl} = 0.05 \sim 0.12$).[42,45] Accordingly, it is considered that until $P_{pl} \approx 0.16$, the superconductivity and TEP are not influenced by the long chain ordering, at least. In spite of the same hole concentration, the T_c for curve B is slightly higher than that for curve A. This seems to suggest that the formation of the CuO chain fragment may enhance the coupling between the CuO_2 planes.

D. Comparison with the hole concentration determined by other techniques: Validity of the present scale

The hole concentration per CuO_2 layer can be chemically estimated from the formal valancy of Cu through the titration technique. From the reported S^{290} and the Cu valency for the double-layer $HgBa_2CaCu_2O_{6+\delta}$ (Hg1212) and triple-layer $HgBa_2Ca_2Cu_3O_{8+\delta}$ (Hg1223) (Refs. 33 and 46), the P_{pl} and the hole concentration per CuO_2 layer determined from the Cu valency P_{CV} are calculated. The P_{CV} of Hg1212 and underdoped Hg1223 are plotted in Fig. 7 as the up- and downward triangles, respectively. In our scale, the optimal doping level for Hg1223 is ~ 0.21 as shown in Sec. III E. In both systems, P_{CV} is almost identical to P_{pl}. In the overdoped side for the triple- and four-layer HTSC, the inhomogeneity charge distribution for inequivalent CuO_2 layers was reported.[47,50] Since our scale was developed for the HTSC with the equivalent CuO_2 layer, we did not use our scale for the Y123 system with chain contribution to TEP. For the same reason we do not apply our scale to the overdoped triple- and four-layer systems. Note also that, for an unknown reason, P_{pl} is not coincident with P_{CV} for the single-layer Hg1201.

The hole concentration per CuO_2 layer for $YBa_2Cu_3O_{6.6}$, $Bi_2Sr_2CaCu_2O_y$ ($T_c = 86$ K), and $Tl_2Ba_2CuO_{6+\delta}$ (Tl2201) with $T_c = 80$ K and 42 K was estimated from the nuclear quadrupole frequency for single- and double-layer HTSCs.[48] The reported hole concentration per CuO_2 layer determined from the nuclear quadrupole resonance (NQR) P_{NQR} is plotted in Fig. 7 as a function of the P_{pl}. The broken line exhibits the $P_{pl} = P_{NQR}$ line. The P_{pl} shows a good correlation with P_{NQR} in the wide doped range from 0.15 to 0.3. According to the relation between Knight shift perpendicular to the *c*-axis and hole concentration for single- and double-layer HTSCs in Ref. 48, we can estimate P_{NQR} for the reported Knight shift data of Hg1201 and Hg1212.[49] The P_{NQR} of Hg1201 and Hg1212 are also plotted in the same figure as the star and upward triangle, respectively. Except underdoped Hg1201 that show some deviation from the $P_{pl} = P_{NQR}$ line, P_{NQR} for both samples also shows good correlation with P_{pl}. The correspondence between P_{pl} and P_{NQR} suggests that the hole concentration macroscopically determined from TEP is consistent with the hole concentration microscopically determined from NQR.

E. Electronic phase diagram by RT scale

We try to validate our scale by examing the pseudogap behavior in various HTSCs. Since the pseudogap state found in ρ (Ref. 3), ARPES,[6] and nuclear magnetic resonance (NMR) experiments[51] has emerged as an intrinsic property of the electronic states of underdoped HTSC, if plotted on a physically meaningful scale, we expect a universal pseudogap behavior for all HTSCs.

First of all, the phase diagram for $Y_{1-x}Ca_xBa_2Cu_3O_y$ (YC123) and Y123 is shown in Fig. 8(a). T_S^*'s for YC1236, YC123 (Ref. 53), $Y_{0.8}Ca_{0.2}Ba_2Cu_3O_y$ ($YC_{0.2}123$) (Ref. 7), and Y123 (Refs. 30 and 41) are found to lie on a common curve that decreases from ~ 300 K at $P_{pl} \approx 0.025$ to ~ 100 K at $P_{pl} \approx 0.24$. T_c's for YC1236, YC123 (Ref. 7), and Y123 (Ref. 11 and 41) also lie on a common curve which appears at $P_{pl} \approx 0.09$ and reaches T_c^{max} at $P_{pl} \approx 0.25$ (curve A in Fig. 6). T_S^* seems to be smoothly connected with T_c at a slightly overdoped level. T_S^* for both curve A and curve B in Fig. 6 lay on the same $T_S^*(P_{pl})$ curve. Another characteristic temperature T_r^*, where ρ exhibits a downward deviation from the *T*-linear behavior, for Y123 (Ref. 3), and YC123 (Ref. 53), form another curve above the T_S^* curve. Noted that T_c's for samples with same structure fall on the same curve and, therefore, for the same structure, T_c can be used as a secondary measure of P_{pl} if S^{290} is not available. Hereafter, we will call temperatures determined by T_r^* and T_S^* as *upper pseudogap temperature* T_{up}^* and *lower pseudogap temperature* T_{lp}^*, respectively. In Fig. 8(b), we plot T_S^*, T_r^* and T_c for CLBC (Ref. 28) and C_xLBLC (Ref. 18) that have crystal structure similar to that of Y123 (Ref. 17). They show tetrag-

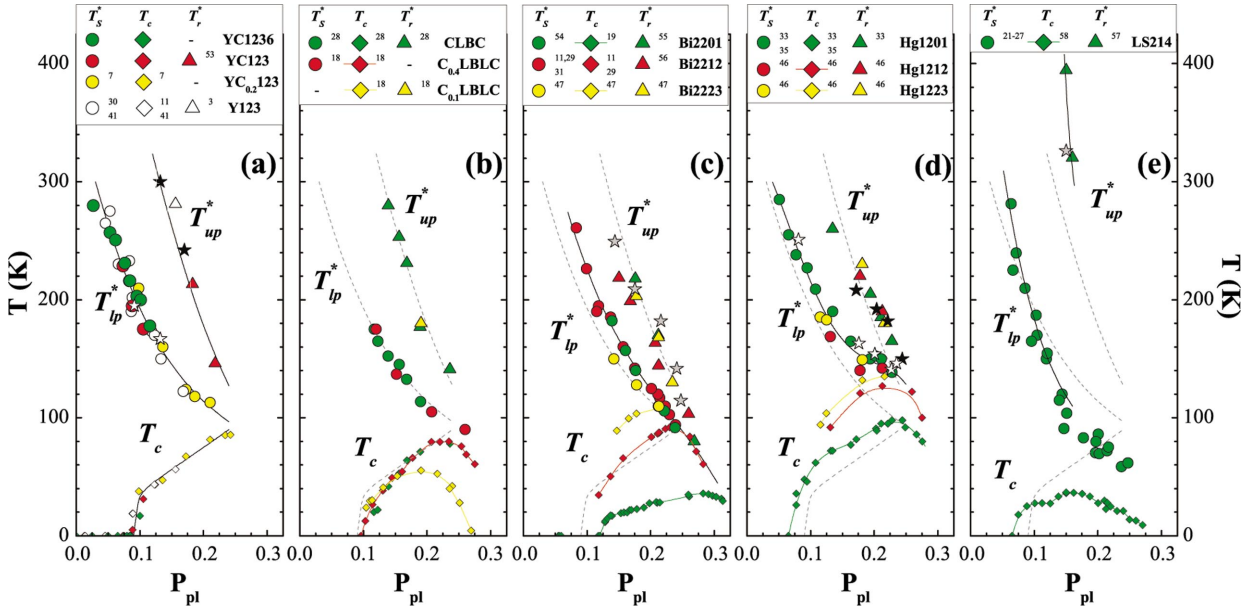

FIG. 8. (Color) T^*_{up} and T^*_{lp} vs P_{pl} in (a) Y123 and YC123, (b) CLBC and C_xLBLC, (c) Bi-based family, (d) Hg-based family, and (e) LS214. All solid lines are a guide to the eyes for T_{up}, T_{lp}, and T_c. The dashed lines represent the same curves as the solid lines for Y123 and YC123. In (a) and (d), the open and closed stars show T^*_s and T^*_{s2} for Zn-substituted Y123 and Zn-substituted Hg1201, respectively (Refs. 32 and 35). In (c) and (e), the gray stars show T^*_{S2} for $Bi_2Sr_2Ca_{1-x}Pr_xCu_2O_8$ and LS214 (Ref. 34).

onal symmetry with no ordered chain. T^*_S and T^*_r fall exactly on the T^*_{lp} and T^*_{up} curves found in Y123 and YC123, respectively. Similar T^*_{up} and T^*_{lp} curves can be obtained for Bi-based family of Bi2201 (Refs. 19, 54, and 55), Bi2212 (Refs. 11, 29, and 56), and $Bi_2Sr_2Ca_2Cu_3O_y$ (Bi2223) (Ref. 47) as shown in Fig. 8(c) and Hg-based family of Hg1201 (Refs. 33 and 35), Hg1212 (Ref. 46), and Hg1223 (Ref. 46) as shown in Fig. 8(d), respectively. This clearly suggests that *two pseudogaps* do not depend on the number of CuO_2 layers in the unit cell. However, the superconductivity is enhanced with increasing number of layers, consistent with the empirical rule of T_c for HTSC. The phase diagram for LS214 is shown in Fig. 8(e).[21–27,57,58] It is seen that *both pseudogaps* follow the universal curves until $P_{pl} \approx 0.15$ where T_c is optimal. It is interesting to note that although our universal P_{pl} scale was originally derived from S[290] of LS214, it does seem that LS214 is an exceptional member of HTSC as commonly believed.

We further demonstrate the possible application and the advantages of using our scale. In Fig. 9(a), we plot the spin-gap temperature signaled by a decrease in ^{63}Cu nuclear relaxation rate $^{63}(T_1T)^{-1}$ with reducing T and the pseudogap

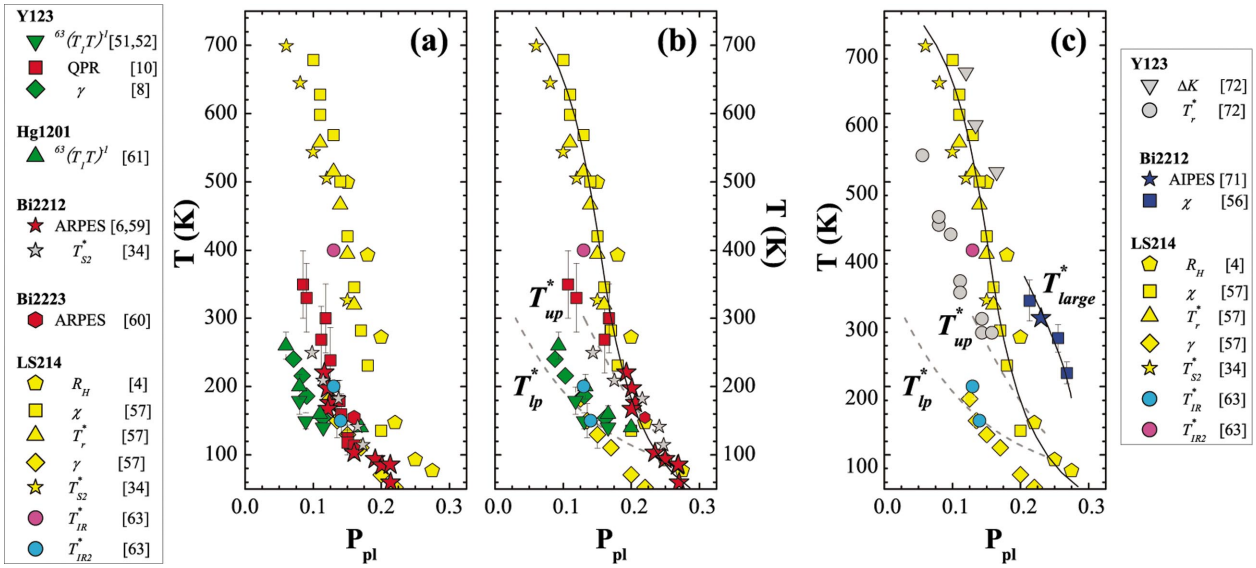

FIG. 9. (Color) Comparison of various characteristic temperatures determined by different probes for different HTSCs as a function of P_{pl} (a) exactly as reported, and (b) and (c) Eqs. (3a) and (3b). For details see text. The T^*_{up} and T^*_{lp} curves (dashed lines) are same as those in Fig. 8. The solid lines are a guide to the eyes.

temperature suggested by the disappearance of leading-edge gap observed by ARPES as a function of P_{pl} exactly as reported in the literature.[6,60,51,52,59–61] There is, except for LS214, no clear distinction among them, and they seem to behave as one pseudogap. However, if we replot the same data using our scale[62] [Fig. 9(b)], the pseudogap and spin gap clearly belong to the T^*_{up} and T^*_{lp}, respectively.

The characteristic temperatures determined from the time-resolved quasiparticle relaxation (QPR) measurement[10] R_H (Ref. 4), and magnetic susceptibility χ (Ref. 57), which are also included in Fig. 9, fall on the T^*_{up} curve. The temperature of a broad peak observed in T dependence of the electronic specific heat coefficient γ falls on the T^*_{lp} curve.[8,9] Thus, various characteristic temperatures, including LS214, belong to either T^*_{up} or T^*_{lp}.

Here, we would like to point out that T^*_{lp} and T^*_{up} are not two temperatures determined by different experimental probes of a common origin. Rather, they have distinct different physical origins. This can be inferred from the suppression of $S(T)$ by Zn substitution below $T^*_{S2}(>T^*_S)$. The T^*_{S2}'s (filled stars) lie exactly on the T^*_{up} curve as shown in Figs. 8(a) and 8(d), while T^*_S (open stars) for the samples substituted until 1% in $YBa_2(Cu_{1-z}Zn_z)_3O_y$ (Ref. 32) and 3% in $HgBa_2(Cu_{1-z}Zn_z)O_{4+\delta}$ (Ref. 35) fall on the T^*_{lp} curve. Further, the T^*_{S2} determined from the $S(T)$ in $Bi_2Sr_2Ca_{1-x}Pr_xCu_2O_8$ and LS214 by another scaling method were plotted into Figs. 8(c) and 8(e) as gray stars, respectively.[34] The same T^*_{S2} for $Bi_2Sr_2Ca_{1-x}Pr_xCu_2O_8$ and LS214 also were plotted into Figs. 9(a) and 9(b) as gray and yellow stars, respectively. T^*_{S2} lies on the upper pseudogap temperature. Therefore, both T^*_{lp} and T^*_{up} are sequentially observed by a single TEP measurement. This result strongly suggests that there are two characteristic temperatures. Another experiment result that we can address is infrared response.[63] The frequency-dependent effective scattering rate $1/\tau$ shows two characteristic temperatures, namely, the temperature T^*_{IR} where the low-frequency $1/\tau$ starts to be clearly suppressed below 700 cm^{-1} and the temperature T^*_{IR2} where the high-frequency $1/\tau$ starts to depend on T. For LS214, the former corresponds to the T^*_{lp} and the latter corresponds to T^*_{up} as shown in Figs. 9(a) and 9(b).

In the optimally doped $La_{1.85}Sr_{0.15}CuO_4$ (P_{pl}=0.15), the ARPES result shows that the pseudogap temperatures were observed beyond ~200 K, although the temperature is much higher than T_c=38 K (Ref 64). This is significantly different from previous results.[6] However, on our phase diagram as shown in Figs. 8(e) and 9(b), the unusual pseudogap temperature at ~200 K belongs to the upper pseudogap temperature, consistent with that observed by ARPES in Bi2212.

Although there are various discussions for double pseudogaps,[65–70] our results provide clear experimental evidence and the calibration (temperature versus carrier concentration) curves of two distinct universal intrinsic pseudogaps in HTSC. The physical origins of *upper* and *lower pseudogaps* have been attributed to the onset of electronic inhomogeneity and superconducting fluctuation, respectively.[66] If we adopt this scenario, our results indicate that both electronic inhomogeneity and superconducting fluctuation in pseudogap regimes are strictly 2D (two dimensional).

Tanamoto *et al.*[70] noticed the two characteristic temperatures observed in Y123: the temperature at which $(T_1T)^{-1}$ versus T takes a maximum (T_R), and the onset temperature of the suppression of $^{89}\Delta K$ (T_S) and studied both temperatures by the extended t-J model.[70] On the present scale, T_R corresponds to the lower pseudogap temperatures.

According to the recent experiment result of ARPES and the angle-integrated photoemission spectroscopy (AIPES) in Bi2212, two types of pseudogap were observed.[71] One is a small pseudogap, the one usually observed by ARPES in Bi2212. The other is a large pseudogap observed only by AIPES. While the small pseudogap temperature touches T_c at a slightly overdoped level, the large pseudogap temperature is much higher than T_c at the same doping level. The large pseudogap by AIPES is plotted in Fig. 9(c) as blue stars. In Bi2212, the third pseudogap temperature was reported in T dependence of the uniform magnetic susceptibility.[56] Further, in Y123, the onset temperature of the suppression of ρ and ΔK above RT was estimated from the T dependence of ρ and ΔK observed below RT by the scaling.[72] Their data also are plotted in Fig. 9(c). On the present scale, it seems to suggest the possible existence of a third pseudogap. Further experimental and theoretical studies are required to pin down the physical origins of these pseudogaps and their behaviors.

IV. SUMMARY AND CONCLUSIONS

In summary, we have shown that $S^{290}(P_{pl})$ of double-layer $Y_{1-x}Ca_xBa_2Cu_3O_6$ follows that of single-layer LS214 and can be represented by Eq. (3). Although it is not clear exactly how this scale works so well, we argued that S^{290} is dictated by some intrinsic equilibrium properties of the electronic states of doped holes and, therefore, can be used as a common scale to measure P_{pl} of layered HTSC cuprates. Indeed, S^{290}'s were found, independent of whether it is doped with hard or soft dopants,[73] to be identical in both $La_2CuO_{4+\delta}$ and $La_{2-z}Sr_zCuO_4$ up to $P_{pl}\approx 0.1$.[74] A universal phase diagram of HTSC is constructed by using our proposed scale of S^{290}. We conclude that for all HTSCs *double pseudogaps* are intrinsically a single CuO_2 layer, and therefore, 2D in nature, property, while T_c depends on interlayer coupling. Most recent experiment results may suggest the existence of a third pseudogap. Our proposed scale points to a unified way to systematically study and compare physical properties of different HTSC and provides further insight into the possible distinct origins of *two pseudogaps*.

ACKNOWLEDGMENTS

One of us (T. H.) would like to thank Dr. K. Yamaya and Dr. K. Kodaira of Hokkaido University, and Dr. S. Yomo of Hokkaido Tokai University for supporting the present research at the initial stage. We are indebted to Dr. Y. S. Song for his technical assistance with TEP measurement. This work was supported by the state of Texas through the Texas Center for Superconductivity at the University of Houston.

*Email address: homma@asahikawa-med.ac.jp

[1] A. Carrington and J. R. Cooper, Physica C **219**, 119 (1994); I. R. Fisher and J. R. Cooper, *ibid.* **272C**, 125 (1996).
[2] H. Yasuoka, T. Imai, and T. Shimizu, in *Strong Correlations and Superconductivity*, edited by H. Fukuyama, S. Maekawa, A. P. Malozemoff, Springer Series in Solid-State Sciences Vol. 89 (Springer-Verlag, Berlin, 1989), p. 254.
[3] T. Ito, K. Takenaka, and S. Uchida, Phys. Rev. Lett. **70**, 3995 (1993).
[4] H. Y. Hwang, B. Batlogg, H. Takagi, H. L. Kao, J. Kwo, R. J. Cava, J. J. Krajewski, and W. F. Peck, Jr., Phys. Rev. Lett. **72**, 2636 (1994).
[5] D. N. Basov, T. Timusk, B. Dabrowski, and J. D. Jorgensen, Phys. Rev. B **50**, R3511 (1994).
[6] H. Ding, T. Yokoya, J. C. Campuzano, T. Takahashi, M. Randeria, M. R. Norman, T. Mochiku, K. Kadowaki, and J. Giapintzakis, Nature (London) **382**, 51 (1996).
[7] C. Bernhard and J. L. Tallon, Phys. Rev. B **54**, 10 201 (1996).
[8] J. W. Loram, K. A. Mirza, J. R. Cooper, and W. Y. Liang, Phys. Rev. Lett. **71**, 1740 (1993).
[9] J. W. Loram, K. A. Mirza, J. R. Cooper, and J. L. Tallon, J. Phys. Chem. Solids **59**, 2091 (1998).
[10] V. V. Kabanov, J. Demsar, B. Podobnik, and D. Mihailovic, Phys. Rev. B **59**, 1497 (1999).
[11] S. D. Obertelli, J. R. Cooper, and J. L. Tallon, Phys. Rev. B **46**, 14 928 (1992).
[12] J. L. Tallon and J. W. Loram, Physica C **349**, 53 (2001).
[13] M. R. Presland, J. L. Tallon, R. G. Buckly, R. S. Liu, and N. E. Flower, Physica C **176**, 95 (1991).
[14] J. L. Tallon, Physica C **168**, 85 (1990).
[15] J. L. Tallon, C. Bernhard, H. Shaked, R. L. Hitterman, and J. D. Jorgensen, Phys. Rev. B **51**, R12 911 (1995).
[16] R. S. Markiewicz and C. Kusko, Phys. Rev. B **65**, 064520 (2002).
[17] D. Goldschmidt, G. M. Reisner, Y. Direktovitch, A. Knizhnik, E. Gartstein, G. Kimmel, and Y. Eckstein, Phys. Rev. B **48**, 532 (1993).
[18] A. Knizhnik, Y. Direktovich, G. M. Reisner, D. Goldschmidt, C. G. Kuper, and Y. Eckstein, Physica C **321**, 199 (1999).
[19] Y. Ando, Y. Hanaki, S. Ono, T. Murayama, K. Segawa, N. Miyamoto, and S. Komiya, Phys. Rev. B **61**, R14 956 (2000).
[20] E. S. Choi, J. S. Brooks, J. S. Qualls, and Y. S. Song, Rev. Sci. Instrum. **72**, 2392 (2001).
[21] Y. Nakamura and S. Uchida, Phys. Rev. B **47**, 8369 (1993).
[22] T. Nishikawa, J. Takeda, and M. Sato, J. Phys. Soc. Jpn. **63**, 1441 (1994).
[23] J.-S. Zhou and J. B. Goodenough, Phys. Rev. B **51**, 3104 (1995).
[24] N. Kakinuma, Y. Ono, and Y. Koike, Phys. Rev. B **59**, 1491 (1999).
[25] D. C. Johnston, J. P. Stokes, D. P. Goshorn, and J. T. Lewandowski, Phys. Rev. B **36**, 4007 (1987).
[26] Z. A. Xu, N. P. Ong, T. Kakeshita, H. Eisaki, and S. Uchida, Physica C **341-348**, 1711 (2000).
[27] Y. Hongjie, W. Bin, Z. Lei, L. Ang, M. Zhiqiang, X. Gaojie, Z. Yuheng, and W. Ye-ning, Physica C **353**, 221 (2001).
[28] K. Hayashi, K. Matsuura, Y. Okajima, S. Tanda, N. Homma, and K. Yamaya, Czech. J. Phys. **46** (S2), 1171 (1996).
[29] M. Akoshima, T. Noji, Y. Ono, and Y. Koike, Phys. Rev. B **57**, 7491 (1998).
[30] J. R. Cooper and J. W. Loram, J. Phys. I **6**, 2237 (1996).
[31] J. B. Mandal, A. N. Das, and B. Gosh, J. Phys.: Condens. Matter **8**, 3047 (1996).
[32] J. L. Tallon, J. R. Cooper, P. S.I.P.N. de Silva, G. V.M. Williams, and J. W. Loram, Phys. Rev. Lett. **75**, 4114 (1995).
[33] A. Yamamoto, W.-Z. Hu, and S. Tajima, Phys. Rev. B **63**, 024504 (2000).
[34] T. Takemura, T. Kitajima, T. Sugaya, and I. Terasaki, J. Phys.: Condens. Matter **12**, 6199 (2000).
[35] A. Yamamoto, K. Minami, W.-Z. Hu, A. Miyakita, M. Izumi, and S. Tajima, Phys. Rev. B **65**, 104505 (2002).
[36] J. R. Cooper, B. Alavi, L-W. Zhou, W. P. Beyermann, and G. Grüner, Phys. Rev. B **35**, 8794 (1987).
[37] R. C. Yu, M. J. Naughton, X. Yan, P. M. Chaikin, F. Holtzberg, R. L. Greene, J. Stuart, and P. Davies, Phys. Rev. B **37**, 7963 (1988).
[38] N. Nagaosa and P. A. Lee, Phys. Rev. Lett. **64**, 2450 (1990).
[39] Here, we exclude compounds with conducting channels other than CuO_2 layer, such as chain layer in fully oxygenated $YBa_2Cu_3O_7$.
[40] T. Honma, K. Yamaya, N. Môri, and M. Tanimoto, in *Proceeding of the 9th International Symposium on Superconductivity, Sapporo*, 1996, edited by S. Nakajima and M. Murakami (Springer, Tokyo, 1997), p. 253.
[41] J. R. Cooper, S. D. Obertelli, A. Carrington, and J. W. Loram, Phys. Rev. B **44**, 12 086 (1991).
[42] M. Akoshima and Y. Koike, J. Phys. Soc. Jpn. **67**, 3653 (1998).
[43] J. R. Cooper, H. Minami, V. W. Wittorff, D. Babić, and J. W. Loram, Physica C **341-348**, 855 (2000).
[44] Y. Wang and N. P. Ong, Proc. Natl. Acad. Sci. U.S.A. **98**, 11091 (2001); cond-mat/0110215v1 (unpublished).
[45] B. W. Veal, H. You, A. P. Paulikas, H. Shi, Y. Fang, and J. W. Downey, Phys. Rev. B **42**, 4770 (1990).
[46] A. Fukuoka, A. Tokiwa-Yamamoto, M. Itoh, R. Usami, S. Adachi, and K. Tanabe, Phys. Rev. B **55**, 6612 (1997).
[47] T. Fujii, I. Terasaki, T. Watanabe, and A Matsuda, Phys. Rev. B **66**, 024507 (2002).
[48] Y. Tokunaga, H. Kotegawa, K. Ishida, G.-q. Zheng, Y. Kitaoka, K. Tokiwa, A. Iyo, and H. Ihara, J. Low Temp. Phys. **117**, 473 (1999).
[49] Y. Itoh, T. Machi, S. Adachi, A. Fukuoka, K. Tanabe, and H. Yasu, J. Phys. Soc. Jpn. **67**, 312 (1998).
[50] Y. Tokunaga, K. Ishida, Y. Kitaoka, K. Asayama, K. Tokiwa, A. Iyo, and H. Ihara, Phys. Rev. B **61**, 9707 (2000).
[51] M. Takigawa, A. P. Reyes, P. C. Hammel, J. D. Thompson, R. H. Heffner, Z. Fisk, and K. C. Ott, Phys. Rev. B **43**, 247 (1991).
[52] A. Goto, H. Yasuoka, and Y. Ueda, J. Phys. Soc. Jpn. **65**, 3043 (1996).
[53] T. Honma, K. Yamaya, N. Môri, and M. Tanimoto, Solid State Commun. **98**, 395 (1996).
[54] Y. Dumont, C. Ayache, and G. Collin, Phys. Rev. B **62**, 622 (2000).
[55] Y. Ando and T. Murayama, Phys. Rev. B **60**, R6991 (1999).
[56] M. Oda, K. Hoya, R. Kubota, C. Manabe, N. Momono, T. Nakano, and M. Ido, Physica C **281**, 135 (1997).
[57] T. Nakano, M. Oda, C. Manabe, N. Momono, Y. Miura, and M. Ido, Phys. Rev. B **49**, 16 000 (1994).
[58] P. G. Radaelli, D. G. Hinks, A. W. Mitchell, B. A. Hunter, J. L. Wagner, B. Dabrowski, K. G. Vandervoort, H. K. Viswanathan, and J. D. Jorgensen, Phys. Rev. B **49**, 4163 (1994).
[59] J. C. Campuzano *et al.*, Phys. Rev. Lett. **83**, 3709 (1999).
[60] T. Sato, H. Matsui, S. Nishina, T. Takahashi, T. Fujii, T. Wa-

tanabe, and A. Matsuda, Phys. Rev. Lett. **89**, 067005 (2002).
[61] Y. Itoh, T. Machi, A. Fukuoka, K. Tanabe, and H. Yasuoka, J. Phys. Soc. Jpn. **65**, 3751 (1996).
[62] Since there is no corresponding S^{290} data except LS214, P_{pl} of all data points plotted in Fig. 9(b) were determined by T_c, our secondary measure of P_{pl}.
[63] T. Startseva, T. Timusk, A. V. Puchkov, D. N. Basov, H. A. Mook, M. Okuya, T. Kimura, and K. Kishio, Phys. Rev. B **59**, 7184 (1999).
[64] T. Sato, T. Yokoya, Y. Naitoh, T. Takahashi, K. Yamada, and Y. Endoh, Phys. Rev. Lett. **83**, 2254 (1999).
[65] B. Batlogg and V. J. Emery, Nature (London) **382**, 20 (1996).
[66] V. J. Emery, S. A. Kivelson, and O. Zachar, Phys. Rev. B **56**, 6120 (1997).
[67] J. Schmalian, D. Pines, and B. Stojković, Phys. Rev. Lett. **80**, 3839 (1998).
[68] R. S. Markiewicz, Phys. Rev. Lett. **89**, 229703 (2002).
[69] D. Mihailovic, V. V. Kabanov, K. Žagar, and J. Demsar, Phys. Rev. B **60**, R6995 (1999).
[70] T. Tanamoto, H. Kohno, H. Fukuyama, J. Phys. Soc. Jpn. **63**, 2739 (1994).
[71] T. Takahasi, T. Sato, T. Yokoya, T. Kamiyama, Y. Naitoh, T. Mochiku, K. Yamada, Y. Endoh, and K. Kadowaki, J. Phys. Chem. Solids **62**, 41 (2001).
[72] B. Wuyts, V. V. Moshchalkov, and Y. Bruynseraede, Phys. Rev. B **53**, 9418 (1996).
[73] B. Lorenz, Z. G. Li, T. Honma, and P. H. Hor, Phys. Rev. B **65**, 144522 (2002).
[74] Z. G. Li, H. H. Feng, Z. Y. Yang, A. Hamed, S. T. Ting, P. H. Hor, S. Bhavaraju, J. F. DiCarlo, and A. J. Jacobson, Phys. Rev. Lett. **77**, 5413 (1996).